PARKES RADIO SOURCES IN THE DIRECTIONS OF SOUTHERN RICH CLUSTERS

DAVID L. BROWN AND JACK O. BURNS
Department of Astronomy, Box 30001/Dept. 4500, New Mexico State University, Las Cruces, New Mexico 88003-0001
Received 31 May 1991; revised 19 August 1991

ABSTRACT

We have compiled a listing of all Parkes radio sources coincident within 0.3 cluster radii of southern rich clusters of galaxies [Abell *et al.* ApJS, 70, 1 (1989)]. A pronounced peak of radio sources very near the cluster centers was found. Bautz Morgan type I clusters tend to have more powerful radio sources and are radio loud ≈ 5 times more often than clusters without dominant central galaxies. There is no strong correlation between radio emission and richness class. We find that the slope of the cluster-radio source two-point angular correlation function is twice that of the galaxy–galaxy correlation function. Furthermore, the correlation amplitude for stronger sources (> 0.65 Jy) is nearly twice that of the entire Parkes catalog sample suggesting a tighter correlation with cluster centers for the stronger sources. Finally, the distribution of spectral indices for Parkes sources within ACO clusters is different from that outside the clusters; stronger cluster sources have steeper spectra on average.

1. INTRODUCTION

Shortly after the publication of the first all northern-sky rich cluster catalog (Abell 1958), a strong relationship between the rich cluster environment and radio emission was recognized. Mills (1960) was first to find a positional correlation between clusters of galaxies and radio sources. Shortly thereafter, van den Bergh (1961) confirmed the findings by Mills with his study of sources from the 3C catalog.

After these initial results, a number of radio surveys (Fomalont & Rogstad 1966; Owen 1974, 1975; Jaffe & Perola 1975; Riley 1975; Colla *et al.* 1975; Mills & Hoskins 1977, and references therein) were made specifically of galaxy clusters. It is now evident that the rich cluster environment has a profound effect on the generation and formation of the radio sources found within. Radio sources residing inside of these rich clusters have more complicated structure and steeper spectral indices than those outside (van den Bergh 1965; Baldwin & Scott 1973; Costain *et al.* 1972; Slingo 1974a,b; McHardy 1979). The probability that a rich cluster galaxy is a radio source has been found to be only weakly correlated at most with the Abell richness class (van den Bergh 1961; Owen 1975; Zhao *et al.* 1989). On the other hand, it has been found that more powerful radio galaxies occur more frequently in Bautz–Morgan type I clusters than in any other type (Wills 1966; Tovmassian & Shirbakyan 1974; Guthrie 1974; McHardy 1974; Owen 1975; Zhao *et al.* 1989). This correlation is most likely caused by the presence of an optically dominant cD galaxy. These cD galaxies are usually the powerful radio sources in the BM type I cluster (Riley 1975).

Sky coverage of the 1958 Abell catalog extended northward of $-27°$ declination. Recently, with the publication of the ACO catalog of southern rich clusters (Abell *et al.* 1989), coverage has now been extended to the southern hemisphere. This new southern catalog now makes further study possible of the radio properties associated with rich clusters.

Recently, two investigations of 408 MHz Molonglo radio sources coincident with the southern ACO clusters were reported (Robertson & Roach 1990; Lustig & Hunstead 1990; hereafter referred to as RR90 and LH90, respectively). Both found an overdensity of Molonglo sources within a projected radius of 100 kpc (for $H_0 = 100$ km s^{-1} Mpc^{-1}) of the cluster centers. RR90 claim this distribution is caused by centrally located dominant cluster galaxies. LH90 showed this hypothesis to be true by studying the morphology of these clusters and optically identifying galaxies associated with the radio emission.

In this paper we investigate the coincidences of radio sources from the well-studied Parkes catalog (Bolton *et al.* 1979) with southern rich clusters. In Sec. 2, descriptions of both the ACO and Parkes catalogs are provided. In Sec. 3, we construct tables listing Parkes radio sources which are coincident within 0.3 Abell cluster radii. Section 4 presents cluster-radio source statistics, where we first consider the overall distribution of Parkes sources within southern Abell clusters and then investigate the two-point angular correlation function between the two. And finally, in Sec. 5, we discuss the implications of our findings with consideration of: (1) potential correlations between richness class and Bautz–Morgan type with those clusters having Parkes sources coincident within 0.3 Abell radii, (2) the run of power at 2700 MHz with BM type, and (3) the frequency distribution of the spectral index.

2. THE CATALOGS

2.1 ACO Catalog

The Southern catalog of rich clusters of galaxies was compiled from the visual study of IIIa-J Southern Sky Survey plates taken by the United Kingdom's 1.2 m Schmidt telescope (hereafter referred to as UKST). This Southern catalog covers the sky south of $-17°$ declination and contains 1364 entries of which two are duplicates and one a repeat in the northern catalog. Clusters were selected which had 30 or more galaxies in the magnitude range m_3 to $m_3 + 2$, with m_3 being the magnitude of the third brightest galaxy. A cluster redshift restriction of $0.02 \leqslant z \leqslant 0.2$ was used in accordance with the nominal completeness of the ACO catalog and further was in agreement with the limits of the Northern Abell catalog. There exists a 10 degree overlap region ($-17°$ to $-27°$) between the Palomar Sky Survey and the

 0004-6256/91/061917-11$00.90

survey done with the UKST. Using 275 Abell clusters found in this overlap zone, ACO compared counts and magnitudes of the southern catalog clusters with Abell's northern clusters. This allowed them to derive relationships that allow comparisons between the southern cluster data and the northern catalog. Within the overlap zone only clusters not listed in the Northern catalog were included in the ACO catalog. Many new clusters have been found in this overlap region and have been included in the ACO catalog since the northern catalog becomes increasingly incomplete near its southern limit. Some important differences in completeness and depth exist between the Abell (1958) and ACO cluster catalogs (Abell *et al.* 1989; Batuski *et al.* 1989; Plionis & Valdarnini 1991).

2.2 Parkes Radio Source Catalog

The Parkes radio source catalog is a collection of major radio surveys done with the Parkes radio telescope (Bolton *et al.* 1979). Figure 1, taken from this same reference, shows the various zones covered by the many surveys along with the flux density levels to which they are complete. Table 1, also taken from the previous reference, lists specific information about each zone and gives references to the original surveys. These surveys were performed at frequencies of 408 and 2700 MHz. Since these original surveys, further observations were made and flux densities were obtained for frequencies ranging from 80 to 22 000 MHz. Currently, the Parkes catalog has radio data for 8263 radio sources.

Nearly all of the sky south of $+27°$ was surveyed with the exceptions of the galactic plane and in the Magellanic cloud regions which were only sparcely sampled. Figure 2 shows an Aitoff projection of the entire Parkes catalog and the projection of a representative model of the Parkes catalog that we constructed for Monte Carlo analysis purposes (see Sec. 4). Further, Fig. 3(a) is the projection of all Parkes sources with flux densities greater than 0.65 Jy at 2700 MHz. This second sample of stronger sources (1409 total) was chosen to provide a statistically complete sample. The constraint of flux densities greater than 0.65 Jy for this subsample is chosen because all of the individual surveys which make up the Parkes catalog are at least complete to this level (see Fig. 1). Figure 3(b) shows a representative model of this smaller complete sample.

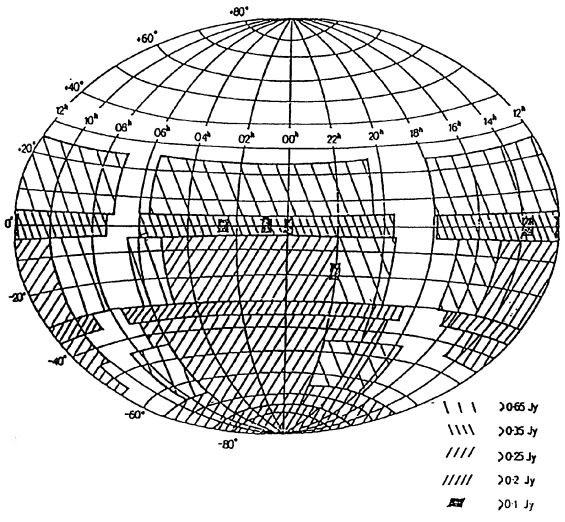

FIG. 1. Completeness levels of the Parkes catalog in various parts of the sky (reproduced from Bolton *et al.* 1979).

3. CLUSTER-RADIO SOURCE COINCIDENCES

For each cluster in the ACO catalog, a computer search was performed through the Parkes catalog to find all the radio sources coincident within 1.0 corrected Abell cluster radii. The Abell radius is (Rudnick & Owen 1977)

$$A_c = \frac{103 q_0^2 (1+z)^2}{q_0 z + (\sqrt{1+2q_0 z} - 1)(q_0 - 1)} \text{ arcsec},$$

with q_0 being the deceleration parameter and z the redshift. This "corrected" radius considers cosmological corrections for the deceleration of the expansion of the universe. The measured redshifts were used if known, otherwise, the redshift was estimated from a piecewise linear relationship between m_{10}, the magnitude of the tenth brightest cluster member, and cz as defined by ACO. Throughout this paper, we assume $H_0 = 75$ km/s/Mpc and $q_0 = 0.1$.

Table 2 lists all ACO clusters which have Parkes radio sources coincident (in projection) within 0.3 Abell radii. The reason for this cutoff at 0.3 Abell radii will be explained later in Sec. 4. Table 3 represents a subsample of Table 2 where only radio sources with flux densities greater than 0.65 Jy at 2700 MHz are considered. This second sample of stronger radio sources was chosen since all the individual surveys which make up the Parkes catalog are at least complete to the 0.65 Jy level at 2700 MHz. For those cases in which a cluster has two or more radio sources coincident with it, the Abell cluster number is repeated for each unique radio source.

The quantities in the columns found in Tables 2 and 3 are defined as follows: (1) Abell catalog number. (2 and 3) R.A. (1950) of Abell cluster. (4 and 5) Dec. (1950) of Abell cluster. (6) B–M—Bautz–Morgan type of Abell cluster (Bautz & Morgan 1970). Colons indicate a mean type, with differences between estimates of two steps, or an uncertain type estimate. Question marks indicate a mean type, with differences between estimates of three or more steps, or a questionable type estimate. (7) M10—Magnitude of the tenth brightest galaxy in the cluster. (8) z clus—Abell cluster redshift where a lower case "m" indicates a measured redshift whereas no designation implies the redshift is an estimate from m_{10}. About 20% of all measured redshifts in the entire ACO catalog are listed as uncertain because of inconsistencies with redshifts derived from m_{10}. However, very few of these redshifts are used in Tables 2 and 3 (with parenthesis denoting those in doubt). (9) R—Richness class. (10) D—Distance class. (11) Radio—Parkes radio source identification. (12) RMT—Radio Morphological Type: compact (CP), narrow-angle tailed (NAT), wide-angle tailed (WAT), double source (DB). References for the radio maps are: (#) Ekers *et al.* 1989; (&) Slee 1977; (%) Christiansen *et al.* 1977. (13) FR—Fanaroff–Riley radio source type (Fanaroff & Riley 1974, hereafter referred to as FR). FR class I sources are edge-darkened (i.e., tailed morphology), low power sources, whereas FR class II sources

TABLE 1. Summary of individual zones of the Parkes 2700 MHz survey S_{lim} is the flux density limit for 95% completeness.

Part No.	Survey Region R.A.	Dec.	Area (sr)	Epoch	S_{lim} (Jy)	No. of sources	Ref.
1	7^h20^m to 17^h50^m 19^h40^m to 6^h	+4° to −4°	0.77	1967-69	0.35	500	W71
2	Selected areas		0.075	1967-69	0.10	311	W71
3	$3^h, 11^h, 19^h, 23^h$	−33° to −75°	0.42	1969-70	0.25	618	S71
4	0^h to 24^h	−75° to −90°	0.21	1970	0.20	454	SB72
5	10^h to 15^h 19^h to 7^h	−35° to −45°	0.59	1970-71	0.25	855	BS73
6	9^h to 16^h30^m 18^h30^m to 7^h15^m	−30° to −35°	0.39	1969-72	0.20	939	SB74
7	8^h to 17^h 19^h30^m to 6^h30^m	−4° to −30°	2.25	1973	0.6	348	B75
8	0^h to 24^h	−65° to −75°	0.37	1972-73	0.25	515	BB75
9	0^h to 3^h 4^h to 8^h30^m 17^h30^m to 19^h 20^h to 23^h	−45° to −65°	0.63	1973	0.6	166	W75
10	7^h to 18^h 20^h30^m to 5^h30^m	+4° to +25°	1.84	1973	0.6	181	S75
11	22^h to 5^h	−4° to −30°	0.79	1973-74	0.25	819	W76
12	22^h to 6^h	−45° to −65°	0.42	1975	0.25	454	W77
13	10^h to 15^h	−15° to −30°	0.32	1976	0.25	404	S77
14	10^h to 15^h	−4° to −15°	0.25	1977	0.25	278	B79

Notes to TABLE 1

S_{lim} is the flux density limit for 95% completeness.
W71—Wall *et al.* (1971).
S71—Shimmins (1971).
SB72—Shimmins & Bolton (1972).
BS73—Bolton & Shimmins (1973).
SB74—Shimmins & Bolton (1974).
B75—Bolton *et al.* (1975).
BB75—Bolton & Butler (1975).
W75—Wall *et al.* (1975).
S75—Shimmins *et al.* (1975).
W76—Wall *et al.* (1976).
W77—Wright *et al.* (1977).
S77—Savage *et al.* (1977).
B79—Bolton *et al.* (1979).

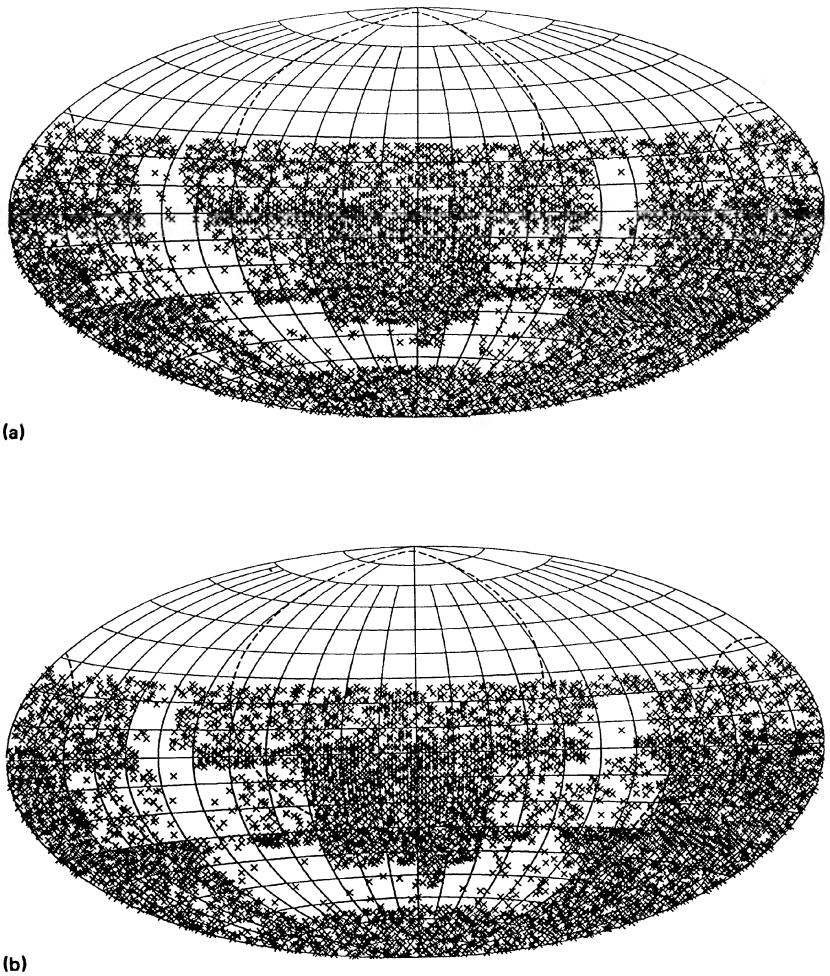

FIG. 2. (a) Aitoff projection of the entire Parkes catalog. (b) Aitoff projection of one of our randomized Parkes catalogs, allowing for differences in completeness levels shown in Fig. 1.

are powerful edge-brightened sources with compact "hot spots" at the lobe extremity. (14) S2700—Flux density in Jy at 2700 MHz. (15) z rad—Radio source redshift if known. (16) SI—Spectral index as determined between 408 and 2700 MHz. For sources not observed at 408 MHz, 5000 MHz flux densities were used to calculate the spectral indices and are indicated by a (*). Those sources with no listed SI are ones which were observed only at 2700 MHz and therefore no spectral index can be calculated. The spectral index is defined as follows:

$$\alpha = \frac{-\ln(S_1/S_2)}{\ln(\nu_1/\nu_2)},$$

where S is the flux density and ν is the frequency. (17) P2700—Power at 2700 MHz. The flux densities were converted into radio powers using the following (Leahy 1991):

$$P_{2700} = 1.91\times 10^{28}\ S_{2700}(1+z)^{\alpha-1} \times [0.1z - 0.9(\sqrt{1+0.2z}-1)]^2\ \text{W/Hz},$$

where S_{2700} is in mJy. For those sources which have no spectral index listed in Tables 2 and 3, an α of 0.7 was used to calculate the powers. (18) l/Ac—This is the distance of the radio source from the Abell cluster center divided by the corrected Abell radius of the cluster. A star (*) immediately following this number indicates that the cluster and radio source are additionally coincident in redshift. We have defined coincidences in redshift as occurring when differences in cluster-radio source redshifts are <0.01, which corresponds to typical velocity dispersions of Abell clusters of 1000 km/s. If an estimated redshift was used for the cluster then an additional allowance was made when looking for coincidences in redshift to account for the larger errors in the estimated redshift. ACO found the spread in the piecewise linear relationship between m_{10} and cz ("c" being the speed of light and "z" the redshift) to be approximately ± 0.3 in log cz.

In Sec. 4 of this paper we explain in detail our reasons for listing only those Parkes sources within 0.3 Abell radii. For now, let us say that at 0.3 Abell radii we found the number of coincident Parkes sources has dropped to the "background" level as determined by Monte Carlo simulations. Those Parkes sources between 0.3 and 1.0 Abell radii are essentially indistinguishable from foreground and background projected sources. However, for a few of these outlying sources we have found an additional coincidence in redshift. Table 4 lists these coincidences. Notice that a classical double source (0618 − 371) is found nearly 0.9 cluster radii away from the center. This is interesting since nearby classical doubles are generally found only in sparse enviroments (Longair & Seldner 1979). This discovery might have interesting conse-

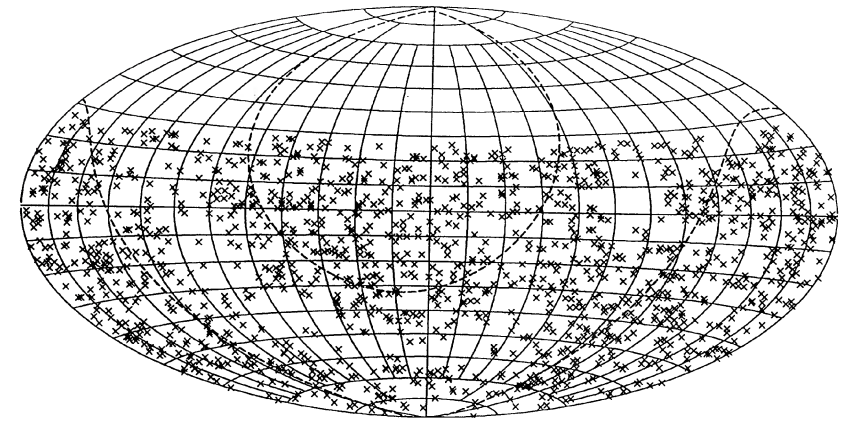

(a)

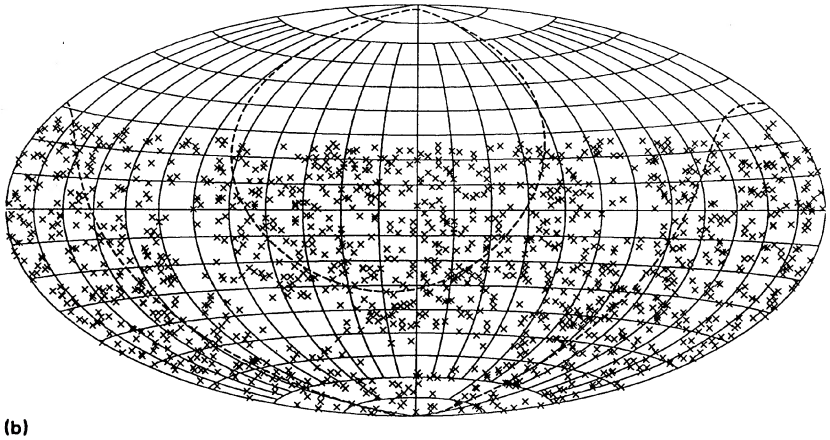

(b)

FIG. 3. (a) Aitoff projection of the complete subsample. (b) Aitoff projection of one of our randomized complete subsamples.

quences for the evolutionary state of the cluster. One could infer that this radio galaxy has not yet fallen into the cluster center, and thus its properties are like that of a noncluster galaxy. This cluster, then, may be dynamically young.

4. CLUSTER-RADIO SOURCE STATISTICS

The number of Parkes radio sources within circular annuli of width 0.1 Abell radii from the cluster centers were counted extending out to one Abell radius. These totals were then divided by the areas of the annuli to give us a number per area for the Parkes sources occurring within the Abell clusters. Figure 4 shows the resulting distribution.

The second histogram in Fig. 4, which is roughly constant, represents the "background level." Because of the nonuniform sampling of radio sources in the Parkes survey, this background was computed using Monte Carlo simulations. We modeled the Parkes radio source catalog to account for the different zones of varying densities resulting from the various surveys from which it is composed. After allowing for the differing densities in certain regions, the model radio sources were then randomly distributed. A typical example of one of our simulations is shown in Fig. 2(b). We generated 100 of these random models of the Parkes catalog, and for each one a cross correlation like that described above was performed with the ACO catalog. For each of the 100 random catalog-ACO cross correlations, we again counted the number of radio sources per unit area for each of the 10 annuli extending from the center of the cluster out to 1 Abell radius. The numbers per area of the 100 random cases were averaged together to produce the roughly constant histogram in Fig. 4 which represents the average number of radio sources that we expect to find to be coincident with the clusters given a purely random distribution. Percentages found with the first four bins indicate the fractional number of sources found in that bin when compared to all sources found within $1.0A_c$.

For the statistically complete sample consisting of only Parkes sources stronger than 0.65 Jy, we again constructed 100 random models in the same fashion as described previously for the entire Parkes catalog [see Fig. 3(b)]. Further, cross correlations were again performed between the ACO catalog and the complete strong source Parkes subsample and the 100 random source catalogs. The results were binned and averaged in the same way as for the entire

TABLE 2. Cluster-radio source coincidences using entire Parkes catalog.

Abell#	RA	DEC	B-M	M10	z clus	R	D	Radio	RMT	FR	S2700	z rad	SI	P2700	1/Ac
2717	0 0.7	-36 14	I-II	15.4	0.0498m	1	3	0000-362			0.220		1.27	1.1E+24	0.055
2719	0 1.4	-23 24	I-II	17.5	0.1196	0	5	0001-233			0.250		0.84	7.4E+24	0.098
2731	0 7.7	-57 16	III:	15.1	0.0312m	0	3	0007-572			0.320		1.03*	6.1E+23	0.041
2741	0 11.2	-32 45	III	18.3	0.1588	1	6	0011-327			0.110			5.8E+24	0.214
2751	0 13.7	-31 40	III	17.6	0.1247	1	5	0013-316	WAT#	I	0.240		0.92	7.9E+24	0.000
2800	0 35.5	-25 22	III	15.6	0.0502	1	4	0035-252			0.280	1.196	-.11*	7.0E+26	0.201
2806	0 37.9	-56 26	I-II	15.1	0.0274m	0	3	0038-564			0.210			3.1E+23	0.096
2809	0 39.1	-44 7	II	18.1	0.1488	0	6	0039-440			0.140			6.5E+24	0.204
2819	0 43.7	-63 52	I-II	15.8	0.0591	2	4	0043-638			0.620		0.53	4.2E+24	0.053
2854	0 58.6	-50 48	I-II	15.6	0.0502	1	4	0058-507			0.610		0.66	3.0E+24	0.000
2860	1 1.8	-40 3	I	16.0	(0.0268)m	0	4	0101-401			0.490		0.67	6.8E+23	0.053
2879	1 8.3	-36 27	II-III?	18.6	0.1749	1	6	0108-364			0.210		0.75	1.4E+25	0.231
2896	1 16.0	-37 22	I	17.4	(0.0317)m	0	5	0116-373			0.080			1.6E+23	0.196
2910	1 23.6	-33 43	II-III:	18.2	0.1537	2	6	0123-337			0.060			3.0E+24	0.085
2959	1 56.4	-50 2	III	18.4	0.1640	0	6	0156-500			0.110		0.52*	6.0E+24	0.180
2978	2 5.9	-32 9	II:	18.0	0.1472	0	5	0206-322			0.150			6.8E+24	0.297
2984	2 9.4	-40 31	I	17.5	0.1196	1	5	0209-405			0.140			4.1E+24	0.000
2995	2 12.9	-25 4	I-II	17.8	(0.0378)m	1	5	0212-248			0.340		0.71*	9.5E+23	0.262
3023	2 26.3	-28 27	III	19.5	0.2338	0	6	0226-284			0.380		0.72	4.6E+25	0.000
3078	2 58.9	-52 2	I	16.8	0.0600m	0	5	0258-520			0.280		0.91*	2.0E+24	0.038
3109	3 14.9	-44 2	I	16.8	0.0673m	0	5	0314-440			0.890		0.54	7.9E+24	0.000
3112	3 16.2	-44 25	I	15.9	0.0703m	2	4	0316-444			0.880		0.67	8.6E+24	0.062
3117	3 19.2	-72 9	II	18.0	0.1472	0	5	0319-721			0.160		0.82	7.3E+24	0.000
3121	3 20.4	-70 40	II	18.0	0.1472	0	6	0320-706			0.230		0.82	1.1E+25	0.000
3125	3 26.0	-53 41	III	15.6	0.0593m	0	4	0325-537			0.110			7.7E+23	0.219
3125	3 26.0	-53 41	III	15.6	0.0593m	0	4	0326-536			0.320		1.59*	2.3E+24	0.159
3135	3 32.2	-39 10	II	15.3	0.0402	2	3	0332-391	WAT#	I	0.940		0.83	3.0E+24	0.000
3142	3 34.9	-39 58	I-II	16.7	0.0858	1	5	0335-399			0.200			3.0E+24	0.074
3151	3 38.4	-28 52	I-II	15.9	0.0616	1	4	0338-288			0.150			1.1E+24	0.055
3153	3 39.1	-34 25	I-II	16.8	0.0895	1	5	0338-343			0.300		0.89	4.9E+24	0.276
3165	3 44.8	-29 11	III	17.2	0.1056	0	5	0344-291			0.490		0.78	1.1E+25	0.125
3223	4 6.6	-30 57	I	15.4	0.0433	2	3	0406-311			0.550		0.64	2.0E+24	0.275
3231	4 11.4	-64 44	II	18.2	(0.0570)m	1	6	0411-647			0.710		0.94	4.6E+24	0.000
3250	4 20.8	-33 22	I-II	18.1	0.1488	0	6	0421-333			0.630		0.75	2.9E+25	0.204
3266	4 30.5	-61 35	I-II	15.3	0.0594m	2	3	0429-616			1.070		0.95	7.6E+24	0.238
3297	4 56.4	-30 13	III	17.1	0.1013	2	5	0456-301	CP&	I	1.580		0.66	3.3E+25	0.060
3300	4 57.9	-24 44	II-III:	18.8	0.1865	1	5	0457-247			0.330		0.70	2.4E+25	0.000
3330	5 13.4	-49 7	II	17.0	0.0903m	1	5	0513-491			0.390		0.75	6.4E+24	0.000
3338	5 21.3	-48 19	II-III	17.3	(0.0446)m	0	5	0521-483			0.610		0.74	2.4E+24	0.168
3341	5 23.7	-31 38	II	14.6	0.0238	2	2	0523-315	WAT#	I	0.190			2.1E+23	0.087
3362	5 40.4	-61 44	I-II	17.1	0.1013	0	5	0540-617			0.470		0.76	9.8E+24	0.000
3363	5 43.8	-47 58	I	17.7	0.1300	3	5	0543-479			0.420		0.64	1.5E+25	0.000
3378	6 4.1	-35 18	I	18.9	0.1927	1	5	0604-352			0.750		0.70	5.9E+25	0.000
3380	6 5.7	-49 29	I-II	15.6	0.0567m	0	4	0605-494			0.610		0.72	3.9E+24	0.000
3391	6 25.2	-53 39	I	16.1	0.0531m	0	4	0625-536			3.700		0.90	2.1E+25	0.034
3392	6 25.3	-35 27	I	15.5	0.0466	1	3	0625-354	CP#	I	2.900		0.53	1.2E+25	0.000
3395	6 26.5	-54 22	II	15.9	0.0498m	1	4	0625-545			1.730		0.78	8.5E+24	0.289
3443	10 18.9	-33 28	II	16.4	0.0758	2	5	1019-334			0.250		1.06*	3.0E+24	0.243
3448	10 26.8	-33 37	II-III	17.8	0.1355	1	5	1026-335			0.140			5.3E+24	0.267
3490	11 42.8	-34 10	I	16.4	0.0758	2	5	1142-341	DB#	I	0.220		0.90	2.6E+24	0.000
3526	12 46.1	-41 2	I-II:	12.9	0.0110m	0	0	1243-412			0.890		0.85	2.1E+23	0.216
3526	12 46.1	-41 2	I-II:	12.9	0.0110m	0	0	1246-410			2.210	0.009	0.83	3.4E+23	0.000*
3528	12 51.6	-28 45	II	15.9	0.0553m	1	4	1251-287			0.300		0.60	1.8E+24	0.050
3532	12 54.6	-30 6	II-III	15.8	0.0591	0	4	1254-300	WAT#	I	0.620		0.84	4.3E+24	0.053
3535	12 55.1	-28 13	III	16.2	0.0698	0	5	1255-282			0.280		0.75	2.7E+24	0.271
3537	12 58.3	-32 10	I-II	13.9	0.0167m	0	2	1257-326			0.230			1.2E+23	0.254
3537	12 58.3	-32 10	I-II	13.9	0.0167m	0	2	1258-321	NAT#	I	0.920		0.62	5.0E+23	0.000
3560	13 29.0	-32 58	I	14.7	(0.0109)m	3	3	1329-328	WAT#	I	0.770		0.85	1.8E+23	0.054
3560	13 29.0	-32 58	I	14.7	(0.0109)m	3	3	1330-328			1.090		0.72	2.5E+23	0.147
3564	13 31.5	-34 58	II	15.3	0.0402	1	3	1331-350			0.150			4.7E+23	0.183
3565	13 33.8	-33 43	I	13.7	0.0109m	1	1	1332-336	WAT&	I	3.230		0.63*	7.4E+23	0.073
3565	13 33.8	-33 43	I	13.7	0.0109m	1	1	1333-336	WAT#	I/II	2.730	0.012	1.33	7.6E+23	0.021*
3565	13 33.8	-33 43	I	13.7	0.0109m	1	1	1334-338			1.800		1.20*	4.1E+23	0.103
3570	13 43.9	-37 40	I-II	15.5	0.0372m	0	4	1343-377			0.510		0.66*	1.4E+24	0.154
3574	13 46.3	-30 3	I	13.0	0.0141m	0	1	1344-302			0.210		0.84	8.1E+22	0.176
3581	14 4.6	-26 47	I	15.2	0.0373	0	3	1404-267			0.500		0.41	1.3E+24	0.000
3595	14 18.0	-86 42	II-III	18.8	0.1865	2	5	1418-867			0.300		0.84	2.3E+25	0.099
3603	14 30.3	-31 35	II-III	15.9	0.0616	0	4	1430-314			0.130			9.8E+23	0.226
3618	15 17.1	-28 23	I	19.3	0.2192	1	6	1517-283			0.610		0.81	6.5E+25	0.000
3626	16 9.9	-83 40	I	17.7	0.1300	0	5	1608-837			0.260		0.68	9.0E+24	0.223
3627	16 11.2	-60 47	I	14.2	0.0143m	1	1	1610-607	WAT%	I	16.80	0.018	1.36*	1.1E+25	0.032*
3628	16 24.6	-75 4	II	18.0	0.1472	1	5	1625-750			0.480		1.08	2.3E+25	0.184
3630	16 33.0	-75 54	I-II	17.5	0.1196	0	5	1633-758			0.110		0.15*	3.0E+24	0.098
3638	19 22.0	-43 3	I-II	17.0	0.0972	2	5	1922-430			0.570		0.71	1.1E+25	0.000

TABLE 2. (continued)

Abell#	RA	DEC	B-M	M10	z clus	R	D	Radio	RMT	FR	S2700	z rad	SI	P2700	l/Ac
3651	19 48.2	-55 13	II	15.4	0.0588m	1	3	1947-551			0.080			5.5E+23	0.235
3654	19 56.0	-35 3	II-III	18.1	0.1488	2	5	1955-350			0.150			6.9E+24	0.166
3678	20 24.1	-31 41	II	18.1	0.1488	1	5	2023-317			0.210		0.83	9.9E+24	0.276
3695	20 31.6	-36 0	I	16.1	0.0669	2	4	2031-359	NAT#	I	0.930		0.82	8.3E+24	0.059
3701	20 34.9	-71 27	I-II	19.1	0.2055	1	6	2035-714			0.220		0.76	2.0E+25	0.151
3706	20 39.0	-38 31	II	16.1	(0.0200)m	0	4	2039-383			0.150			1.2E+23	0.166
3731	20 57.7	-38 51	I-II	17.6	0.1247	0	5	2057-388			0.210		0.80	6.8E+24	0.102
3733	20 59.0	-28 15	I-II	15.4	0.0386m	1	3	2058-282	WAT&	I	3.100	0.038	0.87	8.8E+24	0.097*
3744	21 4.3	-25 41	II-III	14.5	0.0222	1	2	2104-256	WAT#	I	6.200	0.037	0.85	1.7E+25	0.030*
3758	21 17.7	-26 57	II-III	18.1	0.1488	0	6	2117-269			0.590		0.78	2.8E+25	0.144
3785	21 31.0	-53 51	II	16.0	0.0775m	0	4	2130-538			0.780		1.00	9.6E+24	0.096
3799	21 37.0	-72 57	III	15.4	0.0433	1	3	2139-729			0.180			6.6E+23	0.241
3816	21 47.0	-55 33	I-II	15.1	0.0352m	0	3	2148-555			0.870		1.22*	2.1E+24	0.174
3826	21 56.5	-56 24	II	14.9	0.0754m	1	3	2156-564			0.470		0.52	5.3E+24	0.174
3847	22 11.8	-17 16	II-III	19.3	0.2192	0	6	2211-172	CP&	I	4.620	0.153	0.97	2.4E+26	0.112*
3856	22 15.8	-39 9	II-III	17.9	0.1412	2	5	2215-391			0.150		0.95	6.4E+24	0.113
3868	22 18.1	-50 34	II-III	19.2	0.2122	2	6	2218-505			0.760		0.89	7.7E+25	0.154
3879	22 24.1	-69 17	I-II	16.0	(0.0224)m	2	4	2225-694			0.270		-.42*	2.6E+23	0.136
3880	22 25.0	-30 50	II	15.6	0.0502	0	4	2225-308	CP#	I	0.550		0.62	2.7E+24	0.032
3897	22 36.6	-17 39	II	16.6	0.0824	1	5	2236-176	WAT#	I	1.060		0.74	1.5E+25	0.123
3916	22 44.7	-72 11	I-II	17.5	0.1196	0	5	2245-721			0.340		0.78*	1.0E+25	0.278
3936	22 51.2	-35 11	III	18.0	0.1472	2	5	2250-351			0.160			7.2E+24	0.285
3972	23 3.1	-44 38	II-III	17.4	0.1148	1	5	2303-446			0.260		0.89*	7.2E+24	0.201
3985	23 13.3	-23 36	I-II	16.8	0.0895	0	5	2313-236			0.220		0.66	3.5E+24	0.054

Parkes catalog analysis. The resulting histograms are shown in Fig. 5.

As is evident from Figs. 4 and 5, the concentration of Parkes radio sources becomes quite prominent towards the ACO cluster centers. This is consistent with a number of other studies on the distribution of radio sources within clusters (Mills & Hoskins 1977; McHardy 1979; Slee *et al.* 1983; O'Dea & Owen 1985; RR90). Robertson & Roach (1990) suggested that the distribution of Molonglo sources within ACO clusters is best fit by two Gaussians: a narrow, sharply peaked one within 100 kpc and a second broader one from $\approx$100 to $\approx$500 kpc (0.33 Abell radii). However, de Vaucouleurs (1991) has shown that the radial density distribution of Molonglo sources in ACO clusters reported by RR90 follows an $r^{1/4}$ power law and hence a two component distribution may not be necessary. We also find that the stronger Parkes sources are concentrated more tightly near the centers than are those in the entire sample. The strong source sample shows the percentage of Parkes sources per area dropping by nearly 25% when moving from the innermost

TABLE 3. Cluster-radio source coincidences using complete subsample.

Abell#	RA	DEC	B-M	M10	z clus	R	D	Radio	RMT	FR	S2700	z rad	SI	P2700	l/Ac
3109	3 14.9	-44 2	I	16.8	0.0673m	0	5	0314-440			0.890		0.54	7.9E+24	0.000
3112	3 16.2	-44 25	I	15.9	0.0703m	2	4	0316-444			0.880		0.67	8.6E+24	0.062
3135	3 32.2	-39 10	II	15.3	0.0402	2	3	0332-391	WAT#	I	0.940		0.83	3.0E+24	0.000
3231	4 11.4	-64 44	II	18.2	(0.0570)m	1	6	0411-647			0.710		0.94	4.6E+24	0.000
3266	4 30.5	-61 35	I-II	15.3	0.0594m	2	3	0429-616			1.070		0.95	7.6E+24	0.238
3297	4 56.4	-30 13	III	17.1	0.1013	2	5	0456-301	CP&	I	1.580		0.66	3.3E+25	0.060
3378	6 4.1	-35 18	I	18.9	0.1927	1	5	0604-352			0.750		0.70	5.9E+25	0.000
3391	6 25.2	-53 39	I	16.1	0.0531m	0	4	0625-536			3.700		0.90	2.1E+25	0.034
3392	6 25.3	-35 27	I	15.5	0.0466	1	3	0625-354	CP#	I	2.900		0.53	1.2E+25	0.000
3395	6 26.5	-54 22	II	15.9	0.0498m	1	4	0625-545			1.730		0.78	8.5E+24	0.289
3526	12 46.1	-41 2	I-II:	12.9	0.0110m	0	0	1243-412			0.890		0.85	2.1E+23	0.216
3526	12 46.1	-41 2	I-II:	12.9	0.0110m	0	0	1246-410			2.210	0.009	0.83	3.4E+23	0.000*
3537	12 58.3	-32 10	I-II	13.9	0.0167m	0	2	1258-321	NAT#	I	0.920		0.62	5.0E+23	0.000
3560	13 29.0	-32 58	I	14.7	(0.0109)m	3	3	1329-328	WAT#	I	0.770		0.85	1.8E+23	0.054
3560	13 29.0	-32 58	I	14.7	(0.0109)m	3	3	1330-328			1.090		0.72	2.5E+23	0.147
3565	13 33.8	-33 43	I	13.7	0.0109m	1	1	1332-336	WAT&	I	3.230		0.63	7.4E+23	0.073
3565	13 33.8	-33 43	I	13.7	0.0109m	1	1	1333-336	WAT#	I/II	2.730	0.012	1.33	7.6E+23	0.021*
3565	13 33.8	-33 43	I	13.7	0.0109m	1	1	1334-338			1.800		1.20	4.1E+23	0.103
3627	16 11.2	-60 47	I	14.2	0.0143m	1	1	1610-607	WAT%	I	16.80	0.018	1.36	1.1E+25	0.032*
3695	20 31.6	-36 0	I	16.1	0.0669	2	4	2031-359	NAT#	I	0.930		0.82	8.3E+24	0.059
3733	20 59.0	-28 15	I-II	15.4	0.0386m	1	3	2058-282	WAT&	I	3.100	0.038	0.87	8.8E+24	0.097*
3744	21 4.3	-25 41	II-III	14.5	0.0222	1	2	2104-256	WAT#	I	6.200	0.037	0.85	1.7E+25	0.030*
3785	21 31.0	-53 51	II	16.0	0.0775m	0	4	2130-538			0.780		1.00	9.6E+24	0.096
3816	21 47.0	-55 33	I-II	15.1	0.0352m	0	3	2148-555			0.870		1.22	2.1E+24	0.174
3847	22 11.8	-17 16	II-III	19.3	0.2192	0	6	2211-172	CP&	I	4.620	0.153	0.97	2.4E+26	0.112*
3868	22 18.1	-50 34	II-III	19.2	0.2122	2	6	2218-505			0.760		0.89	7.7E+25	0.154
3897	22 36.6	-17 39	II	16.6	0.0824	1	5	2236-176	WAT#	I	1.060		0.74	1.5E+25	0.123

TABLE 4. Cluster-radio source coinicidences with $0.3 < 1/A_c < 1.0$.

Abell#	RA	DEC	B-M	M10	z clus	R	D	Radio	RMT	FR	S2700	z rad	SI	P2700	1/Ac
3004	2 17.0	-48 14	I-II	16.6	0.0635m	0	5	0214-480			1.330	0.064	1.04	1.1E+25	0.804*
3390	6 23.3	-37 19	II	14.7	0.0257	1	2	0618-371	DB#	II	1.800	0.033	0.58	3.8E+24	0.868*
3528	12 51.6	-28 45	II	15.9	0.0553m	1	4	1251-289	DB#	I	0.480	0.056	1.15	3.1E+24	0.397*
3560	13 29.0	-32 58	I	14.7	0.0109m	3	3	1333-336	WAT#	I/II	2.730	0.012	1.33	7.6E+23	0.448*
3593	14 16.4	-19 15	II	16.0	0.1196m	0	4	1417-192			1.100	0.119	0.80	3.3E+25	0.534*

bin to $0.3A_c$, whereas the entire sample has dropped by only 7% at the same point. One can see that in both of our samples, the number of sources per area drops to the "background level" at about 0.3 Abell cluster radii. This is why we chose to list only sources in Tables 2 and 3 which are less than 0.3 Abell radii.

Next, we investigated the two-point angular correlation function between the ACO clusters and the Parkes radio sources for both of our samples. We chose to use an angular measure rather than a linear measure as the independent variable since so few ACO redshifts are known. This correlation function is given by (Bahcall & Soneira 1983; Bahcall *et al.* 1988),

$$w(\theta) = \frac{N(\theta)}{N_R(\theta)} - 1,$$

where $N(\theta)$ is the number of radio sources found within an annulus between θ and $\theta + d\theta$ from the ACO cluster center, and $N_R(\theta)$ is the number of radio sources expected by random chance. In order to compute $N_R(\theta)$, we used the 100 random Parkes catalogs generated for both samples discussed previously. In other words,

$$N_R(\theta) = (1/100) \sum_{i=1}^{100} N_{R_i}(\theta)$$

where we are indexing through the 100 random catalogs. Figure 6 shows the resulting plot of $w(\theta)$ vs θ for the entire Parkes catalog and Fig. 7 for the statistically complete subsample. The error bars shown are calculated assuming Poisson statistics. At large θ values, $w(\theta)$ is symmetrically distributed about zero and no correlation remains.

The lines in each plot are the result of a least-squares linear fit to the first five data points. Only the points out to approximately 8 arcmin were used in the fit since the distribution from that point outward is basically random. The line in Fig. 6 was fit by

$$w(\theta) = (43.91 \pm 1.35)\theta^{-2.04 \pm 0.27}.$$

The line in Fig. 7 was found to fit

$$w(\theta) = (86.84 \pm 1.34)\theta^{-2.17 \pm 0.24}$$

The average corrected Abell radius (A_c) over the entire ACO catalog is 17.6 arcmin. From Figs. 6 and 7, one finds a relatively random distribution starting at about 6.5 arcmin which is slightly over one third of an average Abell radius. This cutoff at one-third agrees with the above analysis and has been found also by RR90 in their study of Molonglo radio sources coincident with ACO clusters.

It is interesting to note that the stronger sources (> 0.65 Jy sample) have an amplitude of correlation which is nearly two times that found for the entire sample. This may suggest that the more powerful sources are more strongly correlated with rich clusters than weaker sources possibly due to the presence of large dominant galaxies in some clusters. Radio power is known to correlate with optical galaxy luminosity (Auriemma *et al.* 1977). This will be pursued further in the next section.

Galaxy–galaxy two point angular correlation functions typically have correlation slopes of -0.67 ± 0.02 and -0.72 ± 0.01 (Picard 1991). Further, Batuski *et al.* (1989) found cluster–cluster correlation slopes of -1.3 ± 0.4 and -1.0 ± 0.2. In our cluster-radio source analysis, we found slopes nearly twice as great, further im-

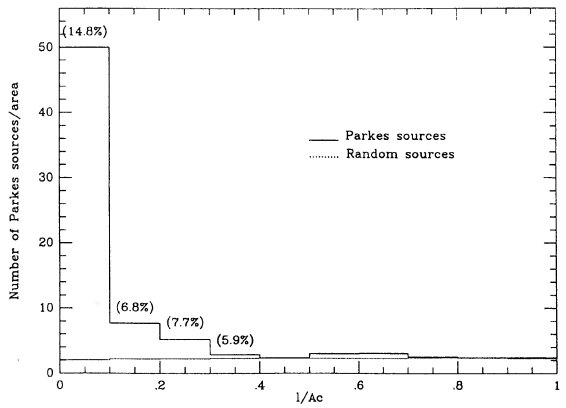

FIG. 4. Distribution of Parkes sources per unit area as a function of distance from the cluster center (in units of Abell radii) for the entire Parkes catalog.

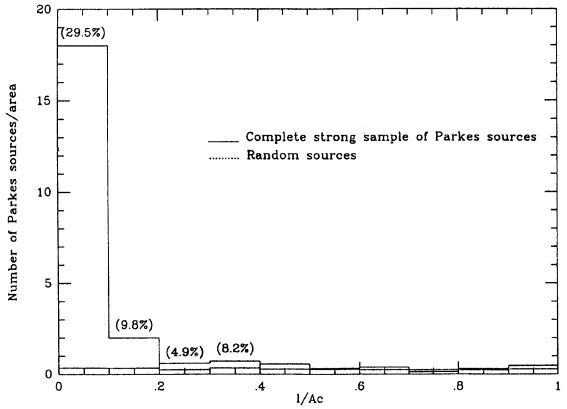

FIG. 5. Distribution of Parkes sources per unit area as a function of distance from the cluster center (in units of Abell radii) for the complete strong source sample.

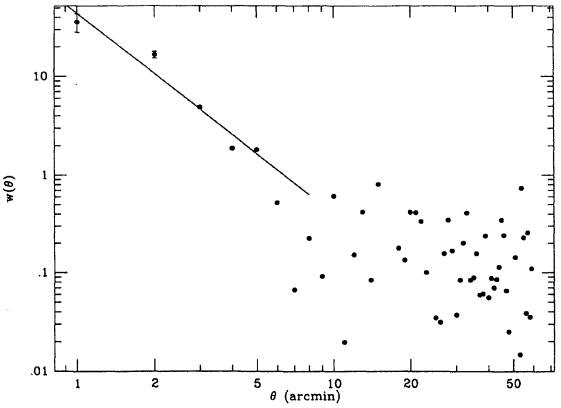

FIG. 6. Two-point angular correlation function between the ACO clusters and the entire Parkes catalog.

plying the very tight association of Parkes sources with ACO cluster centers.

5. DISCUSSION

From Figs. 4 and 5 one can see that the radio source separations from the cluster centers, for both of our samples, are quite small indicating that the radio sources are associated with galaxies very near the cluster center. The question to be asked is whether this enhancement of radio sources near the cluster centers is simply the result of the increased surface density of galaxies or the actual increase of radio sources associated with a central dominant galaxy. To help answer this question we examined the distribution of Bautz–Morgan types in both samples.

Tables 5 and 6, referring to the entire Parkes catalog sample and the stronger source sample, respectively, show the BM type distributions we found. The columns in both tables have the follwng quantities: (1) Bautz–Morgan type of the cluster, (2) number of clusters with given B–M type with radio source within 0.3 radii, (3) total number of clusters with given B–M type in ACO, and (4) percentage detection rate.

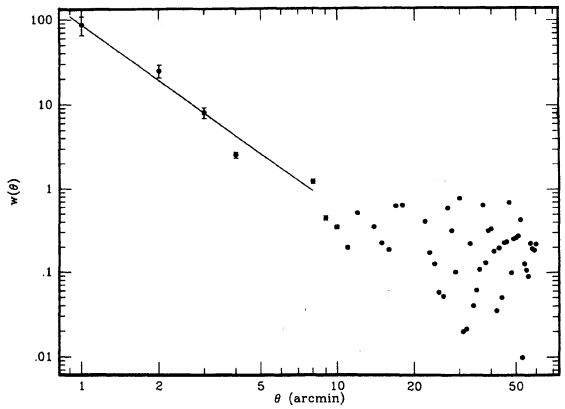

FIG. 7. Two-point angular correltation function between the ACO clusters and the complete subsample of the Parkes catalog.

TABLE 5. B–M type: Entire catalog.

BM	# Found	Total	Percentage
I	19	127	15.0
I-II	25	260	9.6
II	20	249	8.0
II-III	16	367	4.4
III	12	361	3.3

As is evident in Tables 5 and 6, there is a pronounced increase in the frequency of detection of BM type I clusters. Since BM type I clusters are dominated by a single centrally located cD galaxy, it is likely that those radio sources are more often associated with cD galaxies than any other types. This trend is not an obvious richness effect since BM I clusters have a richness distribution similar to other BM types as seen in Table 7. Therefore, we conclude that for at least some of the radio sources near the centers of these rich clusters, these sources are probably physically associated with the central dominant galaxy and are not simply the result of the increased surface density of galaxies near the cluster center. Higher resolution radio observations are needed to confirm these optical identifications.

We further investigated the relationship between the richness class of the cluster and the existence of radio sources within 0.3 cluster radii. For both the entire Parkes catalog sample and the statistically complete subsample made up of the stronger sources, we computed the percentage detection rates for each richness class. The results are shown in Table 8 for the entire Parkes catalog. The columns in Table 8 are as follows: (1) richness class, (2) number of ACO clusters of this richness class with radio sources within 0.3 radii, (3) total number of ACO clusters of this richness class, and (4) percent detection rate. Table 9 shows the results for the strong source sample with columns the same as those in Table 8.

Zhao *et al.* (1989) found weak evidence that richer clusters have a higher probability of radio emission in their study of a complete sample of nearby northern Abell clusters ($D \leqslant 3$). The slight increase in radio detection percentage may be simply explained by the fact that higher richness class clusters contain more galaxies and hence the probability of detection should be higher. For our sample involving the entire Parkes catalog (Table 8), no correlation between richness class and radio emission is found. However, when considering the complete sample of stronger sources (Table 9) there may be a slight increase in the number of ACO clusters with coincident Parkes sources within 0.3 radii as

TABLE 6. B–M type: Complete sample.

BM	# Found	Total	Percentage
I	9	127	7.1
I-II	5	260	1.9
II	5	249	2.0
II-III	3	367	0.8
III	1	361	0.3

TABLE 7. B–M type vs richness class (for ACO clusters).

Richness Class	Bautz Morgan Type I	I-II	II	II-III	III
0	56 (44%)	130 (50%)	102 (41%)	153 (42%)	135 (37%)
1	46 (36%)	91 (35%)	106 (43%)	155 (42%)	156 (43%)
2	20 (16%)	35 (14%)	35 (14%)	53 (14%)	63 (17%)
3	4 (3%)	4 (2%)	6 (3%)	6 (2%)	7 (2%)
4	1 (0.8%)	0 (0%)	0 (0%)	0 (0%)	0 (0%)

TABLE 9. Richness class: Complete sample.

RC	# Found	Total	Percentage
0	7	576	1
1	9	554	2
2	6	206	3
3	1	27	4
4	0	1	0

one moves to richer clusters. But, one should keep in mind that the numbers found here are quite small and therefore the results may not be statistically significant. For example, the first entry in Table 9 (RC 0) has a value and Poisson error of 1.2 ± 0.4, and the third entry (RC 2) has 2.9 ± 1.2.

Next, we considered the distribution of power at 2700 MHz vs BM type. Thus far, we have found the stronger source sample to be more tightly associated with the ACO cluster centers. By looking at Table 3 it is apparent that many of the clusters with stronger sources are of BM type I, I-II, or II. Table 10 shows the percentage distribution of power within six bins. The percentages were computed by dividing the total number of clusters of specified BM type occuring within each power bin by the total number of clusters of that BM type in the entire ACO catalog. The columns are as follows: (1) BM type. (2) Total number of that BM type in Parkes catalog. (3–8) Power bins which are defined in a note to the table. As one can see, the more powerful radio sources occur in BM type I clusters 3–4 times more frequently than in types II-III or III. In particular, the most powerful sources are found in nearly 5% of BM I clusters whereas they are in only $\approx 1\%$ of BM III clusters. Once again, this indicates that optically dominant, central galaxies are more frequently sources of radio emission than other less bright ellipticals (see also, Burns 1990).

Earlier we found the amplitude of the angular correlation function to be nearly twice as great for the stronger source sample. We can now better understand this difference. As we have just found, the early BM type clusters have the most powerful sources, and from Table 3 one can see that all but four of the stronger sources are BM type I, I-II, or II. Additionally, we also found in Figs. 4 and 5 that the stronger sources were more concentrated near the cluster centers than the entire sample.

Finally, we analyzed the distribution of spectral indices for Parkes sources in and out of ACO clusters. Figures 8 and 9 show the results for the entire and the strong source samples, respectively, where we are considering the percentage occurence of spectral indices in bins of 0.1. Notice, first, that both samples of sources within $0.3A_c$ are clearly missing the flat spectrum tail seen in the general distribution of Parkes sources. Second, the mean spectral index and standard deviation (σ) of the α distribution for the entire Parkes catalog are 0.74 and 0.41, respectively, whereas these values for sources occuring within $0.3A_c$ are 0.76 and 0.25. For the strong source sample, we find a mean of 0.66 and a σ of 0.51 when considering all strong sources, and an average α of 0.86 and σ of 0.21 for those within $0.3A_c$. Thus, it appears that the distributions (particularly their widths) of spectral index for sources in and out of ACO clusters are quite different. Since the strongest sources are also more strongly correlated with the ACO cluster centers, one can conclude that these central sources also have steeper spectra on average. This is consistent with higher thermal gas pressures near the cluster centers which are better able to confine extended radio sources and make synchrotron aging of the source spectra more effective (e.g., Roland *et al.* 1976).

6. CONCLUSIONS

Coincidences of Parkes radio sources with southern rich ACO clusters were found and correlations between radio and cluster properties were examined. The results are summarized as follows:

(1) Parkes radio sources are found to reside very near ACO cluster centers. The slope of the ACO-radio source

TABLE 8. Richness class: Entire catalog.

RC	# Found	Total	Percentage
0	39	576	7
1	33	554	6
2	18	206	9
3	2	27	7
4	0	1	0

TABLE 10. Power vs B–M type.

BM	Total #	Percentage found within power bins P_1	P_2	P_3	P_4	P_5	P_6
I	127	0.8	3.1	2.4	3.9	3.1	4.7
I-II	260	0.0	1.9	0.8	4.2	1.9	1.5
II	249	0.0	1.2	0.4	2.0	3.2	1.2
II-III	367	0.0	0.0	0.3	0.8	1.1	1.9
III	361	0.0	0.0	0.8	0.6	1.1	1.1

Notes to TABLE 10

The power bins are as follows:
P_1: $P_{2700} < 1 \times 10^{23}$ W/Hz
P_2: $1 \times 10^{23} \leq P_{2700} < 5 \times 10^{23}$
P_3: $5 \times 10^{23} \leq P_{2700} < 1 \times 10^{24}$
P_4: $1 \times 10^{24} \leq P_{2700} < 5 \times 10^{24}$
P_5: $5 \times 10^{24} \leq P_{2700} < 1 \times 10^{25}$
P_6: $P_{2700} \geq 1 \times 10^{25}$

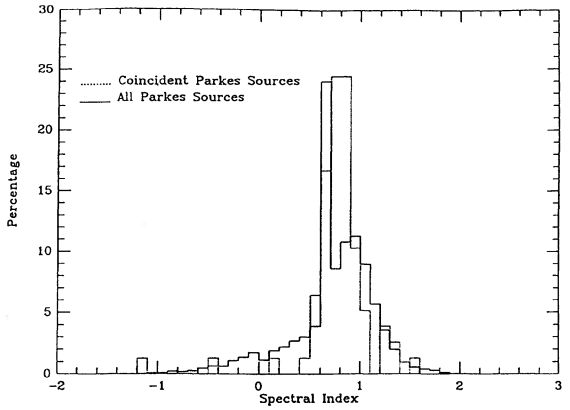

FIG. 8. Distribution of spectral indices for all Parkes sources and those coincident with ACO clusters.

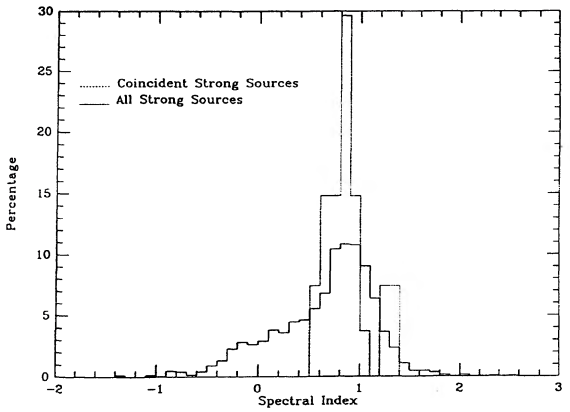

FIG. 9. Distribution of spectral indices for the strong Parkes subsample and those coincident with ACO clusters.

angular correlation function is twice that of the galaxy–galaxy correlation function suggesting a tight coincidence of Parkes sources with the ACO cluster centers. The amplitude of the angular correlation function for the strong sources (>0.65 Jy) is nearly twice that for the overall Parkes sample suggesting an even tighter correlation with the cluster centers for the strongest sources.

(2) Regular clusters (i.e., Bautz–Morgan I to II) are more often sources of radio emission. In particular, BM I clusters contain powerful radio sources ($P_{2700} > 10^{25}$ W/Hz) nearly 5 times more often than BM III clusters.

(3) Parkes sources within ACO clusters have a different distribution of spectral indices than those outside clusters, where the cluster distribution is missing the flat spectrum tail seen in the overall Parkes distribution. Furthermore, the stronger cluster-radio sources have the steepest spectra on average probably due to their association with the dense gaseous environs of the cluster centers.

We wish to thank R. Olowin, F. Owen, and G. Rhee for useful discussions. This work was supported by NSF Grant No. AST90-12353 to J.O.B.

REFERENCES

Abell, G. O. 1958, ApJS, 3, 211
Abell G. O., Corwin H. G., and Olowin R. P. 1989, ApJS, 70, 1
Auriemma, C., Perola, G. C., Ekers, R., Fanti, R., Lari, C., Jaffe, W. J., and Ulrich, M.-H. 1977, A&A, 57, 41
Bahcall, N. A., and Soneira, R. M. 1983, ApJ, 270, 20
Bahcall, N. A., Batuski, D. J., and Olowin, R. P. 1988, ApJL, 333, L13
Baldwin, J. E., and Scott, P. F. 1973, MNRAS, 165, 259
Batuski, D. J., Bahcall, N. A., Olowin, R. P., and Burns, J. O. 1989, ApJ, 341, 599
Bautz, L. P., and Morgan, W. W. 1970, ApJL, 162, L149
Bolton, J. G., and Butler, P. W. 1975, AuJPA, 34, 33
Bolton, J. G., and Shimmins, A. J. 1973, AuJPA, 30, 1
Bolton, J. G., Shimmins, A. J., and Wall, J. V. 1975, AuJPA, 34, 1
Bolton, J. G., Wright, A. E., and Savage, A. 1979, AuJPA, 46, 1
Burns, J. O. 1990, AJ, 99, 14
Christiansen, W. N., Frater, R. H., Watkinson, A., O'Sullivan, J. D., Lockhart, I. A., and Goss, W. M. 1977, MNRAS, 181, 183
Colla, G., Fanti, C., Fanti, R., Gioia, I., Lari, C., Lequex, J., Lucas, R., and Ulrich, M. H. 1975, A&AS, 20, 1
Costain, C. H., Bridle, A. H., and Feldman, P. A. 1972, ApJL, 175, L15
de Vaucouleurs, G. 1991, MNRAS, 249, 28
Ekers, R. D., *et al.* 1989, MNRAS, 236, 737
Fanaroff, B. L., and Riley, J. M. 1974, MNRAS, 167, P31
Fomalont, E. B., and Rogstad, D. H. 1966, ApJ, 146, 528
Guthrie, B. N. C. 1974, Ap&SS, 27, 489
Jaffe, W. J., and Perola, G. C. 1975, A&AS, 21, 137
Leahy, J. P. 1991, Beams and Jets in Astrophysics, edited by Hughes P. A. (Cambridge University Press, Cambridge), p. 110
Longair, M. S., and Seldner, M. 1979, MNRAS, 189, 433
Lustig G., and Hunstead, A. 1990, preprint
McHardy, I. M. 1979, MNRAS, 188, 495
McHardy, I. M. 1974, MNRAS, 169, 527
Mills, B. Y. 1960, AuJPh, 13, 550
Mills, B. Y., and Hoskins, D. G. 1977, AuJPh, 30, 509
O'Dea, C. P., and Owen, F. N. 1985, AJ, 90, 954
Owen, F. N. 1975, ApJ, 195, 593
Owen, F. N. 1974, AJ, 79, 427
Picard, A. 1991, ApJ, 368, L7
Plionis, M., and Valdarnini, R. 1991, MNRAS, 249, 46
Riley, J. M. 1975, MNRAS, 170, 53
Robertson, J. G., and Roach, G. J. 1990, MNRAS, 247, 387
Roland, J., Veron, P., Pauliny-toth, I. I. K., Preuss, E., and Witzel, A. 1976, A&A, 50, 165
Rudnick, L., and Owen, F. N. 1977, AJ, 82, 1
Savage, A., Wright, A. E., and Bolton, J. G. 1977, AuJPA, 44, 1
Shimmins, A. J. 1971, AuJPA, 21, 1
Shimmins, A. J., and Bolton, J. G. 1972, AuJPA, 26, 1
Shimmins, A. J., and Bolton, J. G. 1974, AuJPA, 32, 1
Shimmins, A. J., Bolton, J. G., and Wall, J. V. 1975, AuJPA, 34, 63
Slee, O. B. 1977, AuJPA, 43, 7
Slee, O. B., Wilson, I. R. G., and Siegman, B. C. 1983, AuJPA, 36, 101
Slingo, A. J. 1974a, MNRAS, 166, 101
Slingo, A. J. 1974b, MNRAS, 188, 495
Tovmassian, H. M., and Shirbakyan, M. S. 1974, Afz, 10, 29
van den Bergh, S. 1965, ApJ, 141, 1579
van den Bergh, S. 1961, ApJ, 134, 970
Wall, J. V., Shimmins, A. J., and Bolton, J. G. 1975, AuJPA, 34, 55
Wall, J. V., Shimmins, A. J., and Merkelijn, J. K. 1971, AuJPA, 19, 1
Wall, J. V., Wright, A. E., and Bolton, J. G. 1976, AuJPA, 39, 1
Wills, D. 1966, Observatory, 86, 140
Wright, A. E., Savage, A., and Bolton, J. G. 1977, AuJPA, 41, 1
Zhao, J.-H., Burns, J. O., and Owen, F. N. 1989, AJ, 98, 64